

Lorentz Violation: Loop-Induced Effects in QED and Observational
Constraints

Z. Kepuladze¹

*Institute of Theoretical Physics, Ilia State University, 0162 Tbilisi, Georgia
and Andronikashvili Institute of Physics, 0177 Tbilisi, Georgia*

Abstract

Lorentz invariance is a cornerstone of modern physics, yet its possible violation remains both theoretically intriguing and experimentally significant. In this work, using quantum electrodynamics as an example, we explore how Lorentz invariance violation, introduced into a specific sector of the theory, spreads through loop corrections, modifying the propagation and dispersion relations of other particles. The self-energy and vacuum polarization graphs reveal how LIV effects transfer across sectors, influencing particle kinematics. Due to these loop effects, constraints from cosmic-ray observations and other Earth-based experiments impose limits on induced LIV parameters that would otherwise be less constrained. We show that while interaction-based LIV effects require unrealistically large parameters for detection, modifications to dispersion relations can be probed down to $\delta \sim 10^{-8} - 10^{-9}$ at the LHC. This suggests that accelerator-based resonance studies provide a promising avenue for stringent LIV constraints, potentially rivaling astrophysical observations.

¹zurab.kepuladze.1@iliauni.edu.ge, zkepuladze@yahoo.com

1 Introduction

Lorentz invariance (LI) is a foundational symmetry of the Standard Model and of high-energy physics in general. Because it is so deeply embedded in our theoretical framework, any deviation from exact LI — Lorentz invariance violation (LIV) — would have profound implications for our understanding of nature. Testing this symmetry’s limits is therefore a central goal, both as a precision check of the Standard Model and as a possible window into new physics.

While many LIV searches have placed extremely tight bounds — for example, in the photon, proton and electron sectors — other sectors remain much less constrained. High-energy astrophysical phenomena have long been discussed in this context. The AGASA observations of ultra-high-energy cosmic rays beyond the Greisen–Zatsepin–Kuzmin cutoff [1, 3, 2] and the timing of neutrinos from *Supernova 1987A* have both been interpreted, in some analyses, as potentially allowing for LIV effects in propagation [4]. Threshold reactions such as photon decay [5], vacuum Cherenkov radiation [6], and synchrotron radiation [7], provide remarkably precise constraints in some channels, yet leave significant room for measurable LIV in others. If we are to take a look, the general tendency is that LIV modifications in dispersion relations are much more tightly constrained than those in interactions [8]. These are often expressed in terms of a shift in the maximal attainable velocity c for a given particle species — sometimes colloquially referred to as the “speed of light” for that species. Following the Coleman–Glashow parametrization [9], such a modification can be written as $E^2 - (1 - \Delta c/c)P^2 = m^2$, with $\Delta c/c$ quantifying the deviation. In this work, we will compare our calculations with the existing experimental limits on $\Delta c/c$.

From a broad viewpoint, there are two qualitatively distinct ways LIV could appear at high energy. Either (i) Lorentz invariance is an emergent low-energy approximation that fails at high energy [10], analogous to the relation between relativistic and non-relativistic mechanics (Newtonian mechanics); or (ii) Lorentz invariance is exact in the ultraviolet but becomes broken at lower energies (for example via spontaneous breaking) [11, 12, 13], in which case the violation may be largely superficial and manifest only as small effects, leaving the low-energy theory effectively Lorentz invariant. These broad possibilities motivate the effective field theory (EFT) approach adopted here: introduce representative LIV operators, analyze their consequences, and compare them with experimental constraints, without committing to a specific ultraviolet completion.

A crucial point is that LIV need not be uniform among sectors. Even if initially identical at some high scale, LIV parameters will generally evolve differently under renormalization group running. In gauge theories, this running is closely tied to gauge invariance: if exact GI is absent, LIV effects can be generated or enhanced in specific operators². Conversely, a nominally GI LIV

²While the cited works [14] do not directly address the interplay between LIV and gauge invariance, they do examine general features of renormalization and beta-function running in different, simplified scenarios. These studies highlight that the subject is vast yet incomplete,

operator can, through loop effects, induce gauge-violating structures. This special relation between GI and LIV has been discussed in [11, 12, 15] and will be examined in more detail in Sec. 2. As a result, one may expect a hierarchy among LIV operators at low energies, with a single operator often dominating observable effects. This motivates our strategy of analyzing different operators independently in distinct “what-if” scenarios.

The idea that LIV effects can be transferred between particles and sectors through loop corrections has also been explored in earlier works. For example, in [16], a Chern–Simons term is induced from the vacuum polarization diagram via a specific mass-type LIV operator for the fermion. In [18, 19], various loop effects are analyzed for LIV operators introduced at tree level in GI form. However, as noted above and discussed in more detail in the following section, in the presence of LIV exact GI cannot generally be maintained — the two are intertwined, and one typically implies the breaking of the other. In practical terms, when GI is absent and a single LIV coefficient governs both interaction vertices and kinematic modifications, the resulting observables combine these effects inseparably: one cannot unambiguously attribute the deviation to either the vertex or the propagator alone. Moreover, in many of these works, the photon polarization loop integral is evaluated primarily in the regime $\frac{m_{fermion}^2}{k_{\mu}^2 \text{ ingoing}} > 1$, leaving the high-energy scaling behavior unexplored.

Notably, violations in the kinematic sector can alter the dispersion relations of intermediate particles, opening novel possibilities for detecting LIV in resonance energy regions at high-energy colliders. At the current highest-energy collider, the LHC, many scattering processes proceed via massive intermediate bosons. Since Higgs physics remains relatively new and many related measurements lack precision, studying the weak boson resonance region for possible LIV signatures may be a promising approach in this context.

So, in sec. 2 we introduce the operators and compute loops. In sec. 3 we discuss collider implications and finally we conclude in sec. 4.

2 Calculation of the loop correction

In this chapter, we aim to calculate the “secondary effects” of several LIV operators using quantum electrodynamics (QED) as an example. Let us discuss massless electrodynamics in the Feynman gauge. While massless QED is the technically simpler framework, the qualitative conclusions extend to a wider class of gauge theories. For instance, the fine structure constants of QED and weak interactions are very close to each other. In loop calculations at high energies, mass plays only a secondary role. Clearly, the massless case may spoil the infrared limit; however, when studying LIV effects, the infrared limit is not our primary concern. At the same time, we still provide insight into previously un-

and thus motivate our choice to emphasize general logical conclusions rather than attempt an exhaustive treatment here.

explored high-energy behavior. Before we proceed with this plan, let us expand on the relation between LIV and gauge invariance in a bit more detail.

2.1 LIV vs GI

When considering LIV modifications in a GI setup, it is also important to specify the gauge. If the gauge is not fixed, any LIV operator can effectively serve as a gauge-fixing term and leave the theory Lorentz invariant. A simple example is the mass term $m^2(n_\mu A^\mu)^2$ inserted into an otherwise GI Lagrangian.

Here n_μ denotes a fixed background unit vector that selects a preferred spacetime direction. We normalize it as $n_\mu n^\mu = \pm 1$, depending on whether the vector is time-like ($n_\mu = (1, 0, 0, 0)$) or space-like ($n_\mu = (0, 0, 0, 1)$). In what follows, we treat n_μ as a constant vacuum background in the sense that it does not vary from point to point in spacetime. However, it transforms as a Lorentz vector and only takes the simple component form in a preferred frame, typically associated with the reference frame of distant stars. By contrast, treating n_μ as non-transforming would lead to an unphysical picture.

In the example above, one could perform a gauge transformation to the axial gauge $A_\mu n^\mu = 0$ to eliminate the mass term. In this case, the LIV operator simply fixes the gauge, and the resulting theory remains perfectly Lorentz invariant. The same reasoning applies to interaction terms such as $(A_\mu n^\mu) \bar{\Psi} \not{n} \Psi$ and $(A_\mu n^\mu) \bar{\Psi} \Psi$, where by convention $\not{n} = n_\mu \gamma^\mu$.

More generally, if one introduces operators $F(A_\mu, n_\nu)$, $F(A_\mu, n_\nu) \bar{\Psi} \not{n} \Psi$ or $F(A_\mu, n_\nu) \bar{\Psi} \Psi$, and the corresponding gauge condition $F(A_\mu + \partial_\mu \omega, n_\nu) = 0$ admits a solution for the transformation parameter ω for arbitrary A_μ , then the operator amounts to gauge fixing and does not generate genuine LIV. If no such solution exists, the theory lacks exact gauge invariance and the LIV effects are governed by the non-gauge invariant operator.

A distinct case arises when $F(A_\mu, n_\nu)$ itself has a GI form, e.g. $F(A_\mu, n_\nu) \sim n_\mu F^{\mu\lambda} n^\nu F_{\nu\lambda}$, with $F^{\mu\lambda} = \partial^\mu A^\lambda - \partial^\lambda A^\mu$. This corresponds to an extension of the Lagrangian,

$$\Delta L = \delta n_\mu F^{\mu\lambda} n^\nu F_{\nu\lambda} \quad (1)$$

with δ a LIV parameter, presumably small, but not necessarily so.

For a massless vector field, this modification does not spoil the Lorentz-invariant limit: the field still propagates two degrees of freedom on shell and consistently reproduces the Coulomb law. No apparent contradiction arises at this stage. The situation changes once U(1) symmetry is spontaneously broken in the presence of (1). The vector field then acquires a mass term. Because the setup retains a formally GI structure, one can go to the unitary gauge and calculate the propagator of the massive vector field. There, it becomes clear that the massive vector is over-constrained: instead of three propagating degrees of freedom, as in the LI case, the field still carries only two. This fails to describe a realistic massive vector particle.

The same conclusion follows if we consider two abelian gauge fields with the operator (1) and break symmetry using a complex scalar. One linear combina-

tion becomes massive, while the orthogonal combination remains massless, yet both the massive and massless fields still propagate only two degrees of freedom each. Thus, the degree-of-freedom mismatch persists. The massive vector field still appears over-constrained. We can straightforwardly expand this logic to the electroweak symmetry of the Standard Model, where massive modes again lack the necessary degrees of freedom, and mixing of different fields does not cure the deficit. In summary, while in the unbroken phase the operator (1) shows no immediately obvious inconsistency, once the symmetry is broken the problem becomes explicit: the vector acquires a mass term yet continues to describe only two propagating degrees of freedom instead of three, inconsistent with the structure of a realistic massive vector boson.

This occurs because LIV and GI are so deeply intertwined. In fact, LIV is obscured by gauge degrees of freedom. In [11, 12], it is demonstrated how physical LIV is directly correlated with the size of GI violation. Further research in this matter indicates that gauge theories, both Abelian and non-Abelian, can be obtained by themselves from the requirement of the physical non-observability of the spontaneous LIV [15]. But one may ask, how about LIV operators not directly connected to the vector fields? For example LIV mass type of terms, similar to one considered in [16], $\bar{\Psi} \not{b} \gamma_5 \Psi$ with some prescribed constant vector b^ν . This term is invariant under the global U(1) transformation and henceforth appears manifestly gauge invariant on the surface. However, it breaks not only Lorentz invariance, but also GI as well and this becomes apparent when calculating photon polarization loop taking this modification into account. If $\Pi^{\mu\nu}(p; b)$ denotes the modified photon polarization with external momentum p_λ , then expanding in powers of b^ν gives

$$\Pi^{\mu\nu}(p; b) \approx \Pi_0^{\mu\nu} + \Pi_b^{\mu\nu} + \Pi_{bb}^{\mu\nu}$$

where $\Pi_0^{\mu\nu}$ is the standard GI ($\Pi_0^{\mu\nu} p_\mu = 0$) result. $\Pi_b^{\mu\nu}$ corresponds to a Chern–Simons–like term, which can appear GI in form ($\Pi_b^{\mu\nu} p_\mu = 0$), but is known to be regularization dependent [16], while $\Pi_{bb}^{\mu\nu}$ is no longer gauge invariant, $p_\nu \Pi_{bb}^{\mu\nu} \neq 0$ (See appendix A for proof).

However, one may ask: what does it matter if GI is only broken at second order in b^ν , since such effects might seem practically irrelevant? The important point is that already at linear order the situation is problematic: the induced Chern–Simons term has no unique, regulator-independent value. This ambiguity is well documented in the cited work and subsequent literature [17]. We focused on the self-energy loop diagram because it is central to many discussions of LIV in QED.

Case of the mass term $\bar{\Psi} \not{b} \Psi$ is even simpler. In an otherwise GI setup this term is gauged away by selecting the transformation parameter to be $b_\mu x^\mu$, once again proving the point. One could try to explicitly check higher-order tensor and/or pseudo-tensor structures for fermions, but this would take us farther away from the main goal of the paper, especially when the provided examples paint the picture vividly.

One must state that the same LIV operator may have different effects in differently fixed gauges; they might not be equivalent, and there might not exist

any LIV observable that remains unchanged when moving from one gauge to another. This should not be a surprise, since for LIV to occur, GI violation is necessary, and therefore frameworks with different gauge conditions are not physically equivalent³. Perhaps fixing the gauge in LIV scenarios requires some hard motivation itself, similar to the axial gauge motivated by spontaneous LIV. Whether the Feynman gauge is the optimal choice or is physically the most motivated option is an entirely separate discussion. However, let us abandon that discussion as it is beyond the scope of this paper.

Adopting LIV represents a significant conceptual leap, but quantitatively these effects are expected to be extremely small and exotic. Therefore, any phenomenological model must account for every subtlety, however inconvenient. This is equally crucial experimentally, since data analysis relies heavily on model fitting and any potential LIV signal demands exceptionally careful interpretation given its anticipated small magnitude.

In the framework of massless quantum electrodynamics in the Feynman gauge, let us first analyze the case of LIV interaction and investigate its influence through loop effects on the photon and fermion propagators. Subsequently, we modify the dispersion relation of the photon and the electron and examine their mutual influence on each other. We do not attempt to calculate LIV corrections to the effective vertex, since this part of electrodynamics is the least constrained and cannot provide practically useful limits on LIV parameters.

2.2 LIV interaction

In this section, we first consider the specific scenario in which the leading-order LIV operator modifies the interaction term. Many types of photon–fermion interactions that violate Lorentz invariance could be introduced once higher-dimensional operators are allowed. However, if the LIV background is fixed by a unit vector n_μ and we restrict ourselves to dimension-four operators, only three independent possibilities remain. Two of these were already mentioned above, $(A_\mu n^\mu)\bar{\Psi}\not{n}\Psi$ and $(A_\mu n^\mu)\bar{\Psi}\Psi$, while the third is $(A_\mu n_\nu)\bar{\Psi}\sigma^{\mu\nu}\Psi$ ⁴. The operator $(A_\mu n^\mu)\bar{\Psi}\Psi$, while the simplest, is not very characteristic of vector–fermion interactions. The operator $(A_\mu n_\nu)\bar{\Psi}\sigma^{\mu\nu}\Psi$ resembles a structure typically induced by loop effects, similar to the anomalous magnetic moment, and is therefore

³One might draw a parallel with finite-temperature QFT, which also introduces a preferred rest frame and therefore breaks LI while remaining exactly gauge invariant. However, the analogy has important limitations. Thermal LIV effects originate from ensemble averages of physical degrees of freedom and arise from loop corrections performed in a fixed gauge. These effects are physical and gauge-invariant: the solution (thermal background) lacks the symmetry of the equations, but the gauge structure remains intact. In contrast, in spontaneous LIV the fixed vacuum expectation value is a non-invariant classical solution that does not distinguish between gauge and physical modes. When physical degrees of freedom are isolated, the gauge modes can absorb the would-be LIV, rendering it unobservable unless GI is also broken. Thus, thermal LIV and spontaneous LIV have similar appearances but fundamentally different mechanisms.

⁴Strictly speaking, this classification is not complete. The pseudo-tensor counterparts of these operators are also admissible. However, in massless QED they do not generate linear contributions in two-point loop integrals, and are therefore irrelevant for the present analysis.

expected to be suppressed compared to a primary LIV source. In contrast, the operator $(A_\mu n^\mu) \bar{\Psi} \not{n} \Psi$ has a form consistent with spontaneous LIV. If n_μ represents the vacuum expectation value associated with spontaneous LIV, then $A_\mu n^\mu$ can be interpreted as the Higgs-like mode interacting with the fermion current projected onto the vacuum direction. Thus, it is not an exaggeration to claim that the simplest and physically most motivated choice is

$$\Delta L_{int} = e \delta_{int} (A_\mu n^\mu) \bar{\Psi} \not{n} \Psi \quad (2)$$

The restriction on δ_{int} comes from the covariant derivative form always introduced for fermions, $c^{\mu\nu} \bar{\Psi} (\gamma_\nu D_\mu) \Psi$ to uphold GI. In this construction, $c^{\mu\nu}$ corresponds to our $\delta_{int} n^\mu n^\nu$. For time-like violation, limits for the electron from the clock redshift comparisons and the tests of Einstein equivalence principle lie below 10^{-9} [21], while laboratory bounds from synchrotron and Cherenkov radiation give $4 \cdot 10^{-15}$ [22]. For space-like violation the limits are at the level of 10^{-15} [23]. Some more recent estimates from astrophysical sources are even more stringent, reaching 10^{-19} [24]. While these astrophysical bounds are strict, they often involve assumptions about source modeling or the photon sector, so some caution is warranted. Importantly, these bounds arise from constraints on the electron's velocity shift $\Delta c/c$ and in many cases assume a Lorentz-invariant photon. The limits are then carried over to the interaction constant only because of the shared GI form. Without GI, we do not yet have direct limits on δ_{int} itself. This opens the possibility that, by relaxing the GI assumption, one can derive genuinely new constraints on δ_{int} rather than merely inheriting those tied to $\Delta c/c$. We will explore this possibility below.

2.2.1 Transfer of LIV to fermion kinematics

LIV modifications arise from quantum loop effects, which can alter particle propagation. In particular, self-energy corrections provide insight into how LIV influences the fermion dispersion relation. We now compute the self-energy loop to quantify these modifications. For an incoming momentum p_μ , the self-energy loop calculation is:

$$\begin{aligned} \Pi &= e^2 \int \frac{d^4 q}{(2\pi)^4} (\gamma^\mu + \delta_{int} n^\mu \not{n}) \frac{1}{\not{q}} (\gamma^\mu + \delta_{int} n^\mu \not{n}) \frac{1}{(p-q)_\rho^2} \\ &= -2e^2 (\gamma^\mu (1 + \delta_{int} n_\rho^2) - 2\delta_{int} n^\mu \not{n}) \int \frac{d^4 q}{(2\pi)^4} \frac{q_\mu}{q_\lambda^2 (p-q)_\rho^2} \end{aligned} \quad (3)$$

Here, the photon propagator is taken in the Feynman gauge: $\frac{-i g_{\mu\nu}}{p_\alpha^2}$. Since this integral can only be proportional to p_μ , we define:

$$\int \frac{d^4 q}{(2\pi)^4} \frac{q_\mu}{q_\lambda^2 (p-q)_\rho^2} = p_\mu I_0(p^2) \quad (4)$$

where $I_0(p^2)$ is a divergent integral. Using a simple momentum cutoff with a scale Λ , it can be computed as:

$$I_0(p^2) = -\frac{i}{32\pi^2} \ln \frac{p_\nu^2}{\Lambda^2} \quad (5)$$

In principle, one could find an additional constant alongside the logarithm, depending on the regularization scheme. However, such constants would only redefine the Λ scale without affecting the underlying physics. The divergent part is typically isolated by introducing a scale μ , which does not alter the physical interpretation but reorganizes the expression:

$$I_0(p^2) = -\frac{i}{32\pi^2} \left[\ln \frac{\mu^2}{\Lambda^2} + \ln \frac{p_\nu^2}{\mu^2} \right] = -\frac{i}{32\pi^2} \left[\ln \frac{\mu^2}{\Lambda^2} + I_f \right] \quad (6)$$

where I_f is the finite part. Notably, the division between divergent and finite parts is not uniquely defined at this stage. Thus, Π becomes:

$$\Pi = \frac{i\alpha}{4\pi} (\not{p}(1 + \delta_{\text{int}} n_\rho^2) - 2\delta_{\text{int}}(pn) \not{n}) \left[\ln \frac{\mu^2}{\Lambda^2} + I_f \right] \quad (7)$$

where α is the well-known fine structure constant. Divergent contributions can be eliminated using counter terms, leading to the modified fermion propagator:

$$\begin{aligned} D_f &= \frac{i}{\not{p}} \left(1 + \Pi \frac{i}{\not{p}} + (\Pi \frac{i}{\not{p}})^2 + \dots \right) = \frac{i}{\not{p}} \frac{1}{1 - \Pi \frac{i}{\not{p}}} \\ &= \frac{i \left(1 + \frac{\alpha I_f}{4\pi} \right)^{-1}}{\not{p} \left(1 + \bar{\delta}_{\text{int}} \left(n_\alpha^2 - \frac{4(pn)^2}{p_\alpha^2} \right) \right) + 2\bar{\delta}_{\text{int}}(pn) \not{n}} \end{aligned} \quad (8)$$

Here, $\left(1 + \frac{\alpha}{4\pi} I_f \right)^{-1}$ is the standard renormalization factor, and $\bar{\delta}_{\text{int}}$ is

$$\begin{aligned} \bar{\delta}_{\text{int}}(\mu) &= \frac{\alpha I_f}{4\pi} \delta_{\text{int}} \\ \bar{\delta}_{\text{int}}(\mu_1) - \bar{\delta}_{\text{int}}(\mu_2) &= \frac{\alpha}{4\pi} \delta_{\text{int}} \ln \left(\mu_2^2 / \mu_1^2 \right) \end{aligned} \quad (9)$$

From here on, a bar indicates the loop-induced coefficient for any δ introduced below, as in (9).

From this running we observe that, at lower scales μ , $\bar{\delta}_{\text{int}}(\mu)$ is reduced in magnitude compared to its value at the high scale M_{LIV} . If the highest scale is the LIV scale M_{LIV} (possibly near a GUT scale), then the one-loop contribution at lower energies gives an asymptotic behavior:

$$\bar{\delta}_{\text{int}}(\mu) = \frac{\alpha}{4\pi} \delta_{\text{int}} \ln \frac{M_{LIV}^2}{\mu^2} \quad (10)$$

In our simplified massless-fermion treatment an infrared sensitivity appears in equation (9); however, the infrared energy region $\frac{m_{electron}^2}{p_\mu^2} \gg 1$ is well described by the author in [19], indicating a behavioral change in $\bar{\delta}_{\text{int}}$, with $\bar{\delta}_{\text{int}} \sim E^2$. While the discussed modification pertains to the photon dispersion relation, the general treatment of low-energy behavior still holds. Examining equation (8) we see that the fermion propagator pole is shifted by the loop-induced term, leading to a modified dispersion relation:

$$p_\alpha^2 - 4\bar{\delta}_{\text{int}}(pn)^2 \approx 0 \quad (11)$$

For a given fermion, we observe that $|\Delta c/c| \sim |\bar{\delta}_{\text{int}}|$. The absolute values are used because the sign of $\Delta c/c$ depends on the type of violation and on the sign of $\bar{\delta}_{\text{int}}$. Experimental constraints on electron velocity shifts are stringent, with the strongest limits giving $|\bar{\delta}_{\text{int}}| < 10^{-19}$ [8, 24]. This implies a bound on the underlying interaction parameter of order

$$|\delta_{\text{int}}| < 10^{-16} - 10^{-17}$$

This represents a direct and novel constraint on the interaction strength—one that does not rely on enforcing gauge invariance. A direct comparison with tree-level $c^{\mu\nu}$ -type operators would be misleading, since such terms depend on gauge invariance. In contrast, our framework not only avoids assuming gauge invariance but actively discourages it. Therefore, the constraint derived here reflects a genuinely LIV-induced effect.

This result highlights how LIV in the interaction sector can transmit to fermion kinematics through loops, and how dispersion-relation measurements thus place meaningful constraints on interaction-type LIV operators. In this sense, the present bound is a novel insight: earlier limits reflected only the imposition of gauge invariance, whereas here the restriction emerges directly from LIV effects constrained by electron lightspeed variation.

2.2.2 Transfer of LIV to the photon kinematics

Similar to the fermion propagator, analogous calculations can be performed for the photon polarization fermion loop. If only the Lorentz-violating interaction (2) is employed, the first approximation gives:

$$\bar{\Pi}_{\mu\nu} = \Pi_{\mu\nu} + \delta_{\text{int}}(n_\mu n^\lambda \Pi_{\lambda\nu} + n_\nu n^\lambda \Pi_{\lambda\mu}) \quad (12)$$

where $\Pi_{\mu\nu}$ is the standard expression for electrodynamics [26]:

$$\Pi_{\mu\nu} = (p_\alpha^2 g_{\mu\nu} - p_\mu p_\nu) \Pi_0 \quad (13)$$

This allows us to identify the correction to the propagator as:

$$\Delta D_{\mu\nu} = \frac{-i}{p_\alpha^2} \bar{\delta}_{\text{int}} \left(n_\mu \left(n_\nu - p_\nu \frac{n^\lambda p_\lambda}{p_\alpha^2} \right) + n_\nu \left(n_\mu - p_\mu \frac{n^\lambda p_\lambda}{p_\alpha^2} \right) \right) \quad (14)$$

We should not find strange terms proportional to momentum appearing in the propagator. After all, in the Feynman gauge, the propagator is not manifestly transverse, and besides, such terms do not affect the calculation due to charge conservation. This type of correction does not modify the dispersion relation of the photon. To understand the exact LIV-induced modification in the kinetic operator, one must invert this propagator. An immediate observation suggests that it modifies Coulomb's law for time-like violation case for example; however, this modification is identical to what the interaction (2) itself introduces but with a smaller magnitude:

$$\Delta A_\mu = \Delta D_{\mu\nu} J^\nu = \frac{-i\bar{\delta}_{\text{int}}}{p_\alpha^2} (2n_\mu - p_\mu \frac{n^\lambda p_\lambda}{p_\alpha^2}) n_\nu J^\nu \quad (15)$$

since momentum dependent part does not contribute anyhow in the electromagnetic field.

Corresponding corrections to the kinetic operator follow a similar form to those in the propagator, as expected:

$$\mathcal{K}_{\mu\nu} = i (p_\alpha^2 g_{\mu\nu} - \bar{\delta}_{\text{int}} [n_\mu (p_\alpha^2 n_\nu - p_\nu (n^\lambda p_\lambda)) + n_\nu (p_\alpha^2 n_\mu - p_\mu (n^\lambda p_\lambda))]) \quad (16)$$

In the Feynman gauge, the momentum-dependent part can drop out, leaving an effective correction to the kinetic term of the form

$$\Delta \mathcal{L}_k = 2\bar{\delta}_{\text{int}} (n_\nu \partial_\lambda A^\nu)^2 \quad (17)$$

As already mentioned, this modification does not affect the photon dispersion relation or the speed of light. Therefore, constraints from threshold-energy arguments, Michelson–Morley–type resonator tests, rotating optical cavities, vacuum birefringence, dispersion, or time-of-flight do not apply. Instead, the effects arise only through off-shell photons: a small orientation dependence in static electromagnetic interactions (e.g. LIV corrections to the Coulomb potential for time-like violation or vector potential for general n_μ , and the associated spectroscopic shifts), and polarization-projected distortions in scattering amplitudes and angular distributions.

These contributions mirror those generated by the operator (2), but appear as loop-induced, parametrically suppressed versions of it. In this sense, they inherit the same structure but with reduced magnitude. Importantly, the interaction (2) itself has no direct constraints; the bounds we applied earlier arise only through limits on electron light-speed variation from (11).

2.3 Modification of the dispersion relation of the fermion

If, instead of the LIV interaction (2), the primary source of LIV is a modification of the fermion kinetic operator,

$$\Delta L_f = \delta_f \bar{\Psi} \not{n} (p_\lambda n^\lambda) \Psi \quad (18)$$

then the fermion's dispersion relation is modified in a manner similar to (11). In addition, a dynamical loop effect arises for the photon propagator. The

calculation of the photon polarization operator in this case follows directly from the methods outlined in the previous subsection.

Using the LIV fermion propagator modified by (18), the resulting one-loop perturbation of the photon propagator is:

$$\Delta D_{\mu\nu} = \frac{-ig_{\mu\nu} \bar{\delta}_f (p_\lambda n^\lambda)^2}{p_\alpha^2 \delta_f p_\alpha^2} \quad (19)$$

Such a correction induces the following photon dispersion relation:

$$p_\alpha^2 + \bar{\delta}_f (n^\lambda p_\lambda)^2 = 0 \quad (20)$$

This form is familiar and therefore easier to constrain. Threshold constraints in QED — from processes such as synchrotron radiation, Cherenkov radiation, photon decay, or pair annihilation — primarily restrict the difference between the photon and electron LIV parameters, $\delta_\gamma - \delta_e$, rather than their absolute values. This difference is strongly suppressed, with current bounds $|\delta_\gamma - \delta_e| < 5 \cdot 10^{-21} - 5 \cdot 10^{-22}$ [27].

The implication is twofold: either (i) δ_γ and δ_e are of the same order, in which case both may be much larger than their tiny difference, or (ii) there exists a hierarchy between them, with the larger parameter saturating the bound and the smaller one being effectively unconstrained. Interpreting our loop-induced result, the natural identification is $\delta_e = \delta_f$ and $\delta_\gamma = \bar{\delta}_f$. In this case, we fall into the hierarchy scenario: since $\bar{\delta}_f \ll \delta_f$ (loop suppression), we obtain

$$|\delta_e| = |\delta_f| < 10^{-21} - 10^{-22} \quad (21)$$

and predict a tighter bound for the photon parameter,

$$|\delta_\gamma| = |\bar{\delta}_f| < 10^{-23} - 10^{-24}. \quad (22)$$

2.4 LIV modification of the photon

If the primary source of LIV originates from photon kinematics, the modification to the Lagrangian can be written as

$$\Delta L_{photon} = -\frac{\delta_{ph}}{2} (n^\mu \partial_\mu A_\lambda) (n^\alpha \partial_\alpha A^\lambda) \quad (23)$$

This leads to the modified photon dispersion relation

$$p_\alpha^2 + \delta_{ph} (n^\lambda p_\lambda)^2 = 0 \quad (24)$$

which resembles (20), but differs conceptually: in the present case, LIV arises directly as a primary modification of the photon sector, whereas (20) followed from loop-induced corrections starting in the fermion sector.

Inserting (24) into the fermion self-energy diagram (analogous to (3)), we obtain:

$$\Pi = e^2 \int \frac{d^4 q}{(2\pi)^4} \gamma^\mu \frac{1}{(\not{p} - \not{q})} \gamma^\mu \frac{1}{q_\rho^2 + \delta_{ph} (n^\lambda p_\lambda)^2} \quad (25)$$

Isolating the LIV effect, we find:

$$\begin{aligned}\Pi_{LIV} &= -e^2 \int \frac{d^4 q}{(2\pi)^4} \gamma^\mu \frac{1}{(\not{p} - \not{q})} \gamma^\mu \frac{\delta_{ph} (n^\lambda q_\lambda)^2}{q_\rho^2 q_\alpha^2} \\ &= 2\delta_{ph} e^2 \gamma^\mu \left[I_0 n_\rho^2 p_\mu - 2I_1 (n^\lambda p_\lambda) n_\mu + I_2 p_\mu \frac{(n^\lambda p_\lambda)^2}{p_\alpha^2} \right]\end{aligned}\quad (26)$$

where I_i are loop integrals evaluated using Feynman parametrization:

$$I_0 = \frac{1}{4} \int_0^1 dx \int \frac{d^4 q}{(2\pi)^4} \frac{x^2 q_\rho^2}{(q_\rho^2 + x(1-x)p_\alpha^2)^3} = \frac{-i}{384\pi^2} \left(\frac{1}{2} + \frac{13}{3} \ln \frac{p_\nu^2}{\Lambda^2} \right) \quad (27)$$

$$I_1 = \frac{1}{4} \int_0^1 dx \int \frac{d^4 q}{(2\pi)^4} \frac{x(1-x)q_\rho^2}{(q_\rho^2 + x(1-x)p_\alpha^2)^3} = \frac{-i}{384\pi^2} \left(\frac{1}{4} + \frac{5}{3} \ln \frac{p_\nu^2}{\Lambda^2} \right) \quad (28)$$

$$I_2 = p_\alpha^2 \int_0^1 dx \int \frac{d^4 q}{(2\pi)^4} \frac{x^2(1-x)^2}{(q_\rho^2 + x(1-x)p_\alpha^2)^3} = \frac{i}{192\pi^2} \quad (29)$$

Here x is the Feynman parameter and Λ is the cutoff scale, as before. Among these, I_0 and I_1 are logarithmically divergent, while I_2 is convergent. The divergent parts can be absorbed by counterterms; after introducing a renormalization scale μ , one finds

$$\Pi_{LIV} = 2\delta_{ph} e^2 \gamma^\mu \left[\left(I_0 n_\rho^2 + I_2 \frac{(n^\lambda p_\lambda)^2}{p_\alpha^2} \right) p_\mu - 2I_1 (n^\lambda p_\lambda) n_\mu \right] \quad (30)$$

$$= \frac{-i\delta_{ph}\alpha}{24\pi} [\mathcal{A}(p) \not{p} - \mathcal{B}(p) (n^\lambda p_\lambda) \not{n}] \quad (31)$$

where

$$\mathcal{A}(p) = n_\rho^2 \left(\frac{1}{4} + \frac{13}{6} \ln \frac{p_\nu^2}{\mu^2} \right) - 2 \frac{(n^\lambda p_\lambda)^2}{p_\alpha^2} \quad (32)$$

$$\mathcal{B}(p) = \frac{1}{4} + \frac{5}{3} \ln \frac{p_\nu^2}{\mu^2} \quad (33)$$

From this, we can define the modified fermion propagator:

$$\begin{aligned}D_f &= \frac{i}{\not{p} - \not{p} \Pi_{LIV} \frac{i}{\not{p}}} = \\ &= \frac{i \left(1 - \frac{\delta_{ph}\alpha}{24\pi} (\mathcal{A}(p) + 2(p^\alpha n_\alpha) \frac{\mathcal{B}(p)}{p_\mu^2}) \right)^{-1}}{\not{p} + \frac{\delta_{ph}\alpha}{24\pi} \mathcal{B}(p) (p^\alpha n_\alpha) \not{n}} \Rightarrow \frac{i}{\not{p} + \bar{\delta}_{ph} (p^\alpha n_\alpha) \not{n}}\end{aligned}\quad (34)$$

thus:

$$\bar{\delta}_{ph} = \delta_{ph} \frac{\alpha \mathcal{B}(p)}{24\pi}$$

Once again, loop corrections transfer LIV between the photon and fermion sectors, producing modified fermion propagation and dispersion. The structure of the result is similar to the previous subsection, but the origin is different. Experimental constraints on $|\delta_\gamma - \delta_e|$ again enforce a hierarchy between photon and fermion parameters, leading to

$$|\delta_\gamma| = |\delta_{ph}| < 10^{-21} - 10^{-22}, \quad |\delta_e| = |\bar{\delta}_{ph}| < 10^{-23} - 10^{-24} \quad (35)$$

In this case, however, the hierarchy is inverted relative to the scenario where the fermion LIV was primary.

3 About accelerator specific physics

Experimental and observational data overwhelmingly show that modifications to kinematics and dispersion relations are measured with far greater precision than modifications to interactions. Beyond the constraints derived from cosmic-ray threshold energies and other astrophysical observations, high-energy scattering processes in accelerators provide a unique and sensitive avenue for detecting LIV effects — particularly when intermediate bosons are involved. If the center-of-mass energy of an experiment is sufficiently high, LIV-induced modifications to intermediate boson dispersion relations become especially relevant.

In the works [28, 29] LIV modifications in the quark sector were analyzed in the context of the LHC. The modifications to cross sections depend on the relative orientation of the scattering process (correspondingly, the orientation of the proton–proton collision axis and detector) with respect to the preferred direction of LIV. If this direction is fixed by a vector n_μ (similar to our previous notations), then, in simplified form, the Drell–Yan cross section can be written as

$$\frac{d\sigma_{LIV}}{dM^2} = \frac{d\sigma_{LI}}{dM^2} \left(1 + \delta_i \frac{E_i^2}{M^2} f_i(\Omega, n)\right) \quad (36)$$

where Ω symbolically denotes the orientation of the process in space, f_i are specific functions of Ω and n_μ and δ_i are small LIV parameters (not related to any parameters introduced in previous sections). Here E_i is the particle energy and M is so-called invariant mass.

Since the Earth rotates — and with it the LHC — the orientation Ω changes with time, so an anisotropy should appear in the measured cross sections. Although this result was calculated for a specific type of LIV modification, the functional form is rather general and applies to a broad class of LIV operators, including those of the type (2) in leading approximation. The constraints $\delta_i < 10^{-5}$ obtained from cross-section analyses can thus be generalized to any such δ_i provided there is no significant energy dependence.

The prefactor E_i^2/M^2 , while indicating the expected scaling of LIV effects with energy, is not a large ratio in this analysis. This is partly because the final-state particles typically carry significantly less energy than the full center-of-mass energy, and partly because events with sizeable E_i^2/M^2 are rare and require especially careful treatment. Even then, only small pseudo-rapidity

regions $|\eta| < 2.4$ were considered. Improving on these points could yield much better sensitivity to LIV effects, since values like $\delta_i \sim 10^{-5}$ may already be unrealistically large. This argument is supported by loop calculations in this and previous work [18, 19], although many explicit computations were performed in simplified QED settings, the qualitative parametric behaviour — namely that a loop-generated coefficient is suppressed by a factor $\frac{\alpha}{4\pi}$ relative to a tree-level parameter — is generic and continues to hold in the presence of masses. For massive intermediate bosons this loop factor controls the induced coefficient, while threshold and finite-mass effects modify only the numerical prefactor and the scale dependence (logs such as $\ln \frac{M_{LIV}}{M_B}$). So, general outcome holds and LIV effects are transmitted to other sectors, with LIV parameters suppressed by loop factors (proportional to the relevant fine-structure constants). Because the weak and QED fine-structure constants are numerically close, any LIV parameter as large as $\delta_i \sim 10^{-5}$ would induce unacceptably large corrections in the weak sector and thereby in all stable particles.

In light of these considerations, the most promising chance for detecting LIV effects lies in massive intermediate bosons, since they carry the largest energies in scattering processes. If LIV modifies the dispersion relation of such a boson — as in (24) — the consequences for resonance physics are pronounced:

$$p_\alpha^2 + \delta_B (n^\lambda p_\lambda)^2 = M_B^2 \quad (37)$$

where M_B is the boson mass. Although this form looks directly motivated by (24), it is in fact one of only two renormalizable modifications compatible with a fixed n_μ . The alternative,

$$p_\alpha^2 + m_B (n^\lambda p_\lambda) = M_B^2 \quad (38)$$

with small LIV parameter m_B , produces a much weaker energy scaling and is therefore harder to detect. At the same time accepting (24), makes its easy to consider the form (37) for the weak bosons specifically (with a certain level of fine-tuning), because whatever origin of LIV may be photon is still mixed state of $U(1)_y$ and $SU(2)$ gauge bosons.

Proceeding with this choice, the resonance behavior is significantly modified, since both the resonance mass and width are governed by

$$p_\alpha^2 = M_{B,eff}^2 = M_B^2 - \delta_B (n^\lambda p_\lambda)^2 \quad (39)$$

This effective mass picture has immediate experimental consequences. For example, if the decay rate is modified as [13],

$$\Gamma_{LIV} = \frac{M_{B,eff}^2}{M_B^2} \Gamma_{LI} \quad (40)$$

then the unstable boson propagator becomes

$$\begin{aligned} D_B &= \frac{i}{p_\alpha^2 - M_B^2} \rightarrow \frac{i}{p_\alpha^2 - (M_{B,eff} - ip_0 \Gamma_{LIV}/2M_{B,eff})^2} \\ &= \frac{i}{p_\alpha^2 - M_{B,eff}^2 (1 - i\Gamma_{LI}/2M_B)^2} \end{aligned} \quad (41)$$

Consequently, the scattering cross section involving this intermediate boson is proportional to:

$$\sigma_B^{LIV} \sim |D_B|^2 \quad (42)$$

From this, we find for the resonance mass and peak cross section:

$$M_{res}^2 = M_{B,eff}^2 (1 - \Gamma_{LI}^2 / 4M_B^2) \quad (43)$$

$$\sigma_{B,max}^{LIV} = \sigma_{B,max}^{LI} \frac{M_B^2}{M_{B,eff}^2}, \text{ since } \sigma_{B,max}^{LI} \sim \frac{1}{\Gamma_{LI}} \quad (44)$$

Applying this framework to the weak Z boson and comparing the resonance mass shift with the current precision of M_Z , $|\Delta M_Z| = |M_Z - M_{Z,resonance}| \approx 2$ MeV [30], using (39) for timelike n^λ , we estimate at LHC energies, $E = 14$ TeV

$$|\delta_B| \approx \frac{2M_Z |\Delta M_Z|}{E^2} \approx 2 \cdot 10^{-9} \quad (45)$$

If LIV is present, then the data actually follow the LIV-modified distribution σ_B^{LIV} . Fitting the same data under the LI assumption still yields a fit, but with shifted parameters. For example, generating data with $\delta_B = -2 \cdot 10^{-9}$ at energies 14 TeV— using the Z boson mass and decay rate — and fitting it with the LI form results in a shift of $\Delta M_Z \approx -2$ MeV (expected number according to (45)) in the resonance peak of the perceived LI cross section, while the decay rate remains largely unaffected.

The sign and magnitude of this shift depend both on the sign of δ_B and on the energy of the process. To demonstrate the difference between LI and LIV cross sections, we can plot the relative deviation $\Delta\sigma/\sigma = (\sigma^{LIV} - \sigma^{LI})/\sigma^{LI}$. This provides a robust comparison, as it does not rely on the exact form of the cross section but rather on the ratio of LIV to LI propagators. Thus, we obtain:

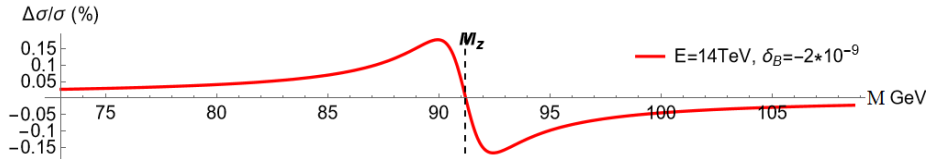


Figure 1: Relative deviation $\Delta\sigma/\sigma$ as a function of the invariant mass of the Z resonance is plotted for $E = 14$ TeV and $\delta_B = 2 \times 10^{-9}$. The vertical dashed line marks the Z-boson mass M_Z . LIV effects are nonzero at M_Z and reach a maximum of about 0.17% around 1.2 GeV away from the M_Z value.

This shows that LIV effects are maximal near the resonance region, where the LIV deformation competes with the mass term, and decrease away from it, where LIV scales like the dominant contribution and gives only a fractional correction of order δ_B .

The resonance line shape also depends on the total center-of-mass energy through the effective mass of the intermediate boson. At larger energies, the

deformation becomes more pronounced, and the perceived resonance position is shifted further from the true mass. For processes with lower center-of-mass energy—close to the boson mass—the resonance aligns with the real mass, and LIV distortions become negligible.

In proton–proton collisions, the intermediate gauge bosons are produced with a broad distribution of energies defined by parton distribution functions. High-energy bosons, which would exhibit stronger LIV effects, are produced much less frequently, leading to a dilution of the observable LIV signal when all events are combined. To make the picture more explicit, we rewrite the kinematics in the standard Drell–Yan variables. Using the invariant mass M and boson rapidity Y , the momentum can be parametrized as

$$p_\alpha = M(\cosh Y, \vec{r} \sinh Y), \quad p_\alpha p^\alpha = M^2 \quad (46)$$

where vector \vec{r} defines an axis of collision. For a timelike n^λ the effective LIV-modified mass becomes

$$M_{B,eff}^2 = M_B^2 - \delta_B M^2 \cosh^2 Y \quad (47)$$

and the position of the resonance shifts to

$$M_{res}^2 \approx M_B^2(1 - \delta_B \cosh^2 Y) - \Gamma_{LI}^2/4 \quad (48)$$

Thus, the deformation grows approximately like $\cosh^2 Y$, and reaches its largest values at high rapidity. At the LHC, rapidities up to $Y \approx 5$ are kinematically allowed (defined from the $Y_{\max} = \ln(E/M_z)$), but events with such large Y are rare. This naturally motivates a search strategy based on rapidity (energy) segregation: low-rapidity samples determine the physical mass, while high-rapidity subsets isolate potential LIV-induced deviations. Given the rapidity-dependent nature of LIV-induced resonance shifts, screening high-rapidity processes near the resonance region provides a distinct signature that can be disentangled from Standard Model backgrounds, which typically lack such specific kinematic dependence.

This suggests that accelerator experiments, if analyzed carefully, can be more sensitive to LIV than previously thought — potentially on par with cosmological bounds on neutrinos, $\Delta c/c \sim 10^{-8} - 10^{-9}$.

Of course, this is not a full analysis and a more detailed investigation involving strict calculations of Drell–Yan processes is needed for definitive conclusions. Nevertheless, this preliminary estimate highlights a promising avenue for LIV searches, suggesting that collider studies may offer constraints comparable to or even surpassing astrophysical observations. This is even more interesting in the context of recent tension between measurements of the weak W -boson mass by Tevatron and LHC, being outside of each other’s range of accuracy [31, 32]. It is unclear yet whether this tension is genuine or product of the mistake or bias, but if there is a merit to it, it is consistent with LIV behavior.

4 Conclusion

Lorentz invariance is a foundational principle of modern physics, yet the possibility of its violation remains an intriguing direction for theoretical exploration and experimental investigation. In this work, we analyzed how LIV, when introduced into one sector of the theory, propagates through loop corrections, affecting particle propagation and dispersion relations. Using self-energy and vacuum polarization graphs, we demonstrated how LIV influences kinematics, leading to measurable effects even when initially suppressed.

Experimental constraints from cosmic-ray observations, neutrino astrophysics, and high-energy collider studies impose limits on these induced LIV parameters. While direct interaction-based LIV effects would require unrealistically large values for detection, modifications to dispersion relations offer a more promising route. In particular, accelerator-based resonance studies can probe LIV down to $\delta \sim 10^{-8} - 10^{-9}$. A full process-specific cross-section calculation is an interesting next step and is currently being considered; however, the resonance-shift effect described here is essentially model-independent and therefore provides a robust target for collider studies.

Our findings emphasize the interconnected nature of LIV effects, showing that even when introduced in a specific sector, they inevitably spread across others via quantum loops. This underlines the importance of considering secondary effects when evaluating LIV constraints. Looking ahead, a deeper examination of Drell–Yan processes and precision resonance measurements at future collider experiments could further refine these bounds and provide valuable insights into the viability of LIV in fundamental physics.

5 Acknowledgments

This research is financed by SRNSF (*grant number: STEM-22-2604*). I would like to thank Jon Chkareuli and Juansher Jejelava for useful discussions.

Appendix A: Gauge invariance breaking in the modified photon polarization loop

The polarization diagram modified by the LIV axial mass term is given as follows:

$$\Pi^{\mu\nu}(p; b) = \int \frac{d^4q}{(2\pi)^4} \text{Tr}[\gamma^\mu S(q) \gamma^\nu S(q-p)], \quad (49)$$

with $S(k) = 1/(k - b\gamma^5)$. We can assume b^ν to be small and expand in the series with respect to b^ν up to the second order. We also neglect the mass term

for the fermion. These assumptions will have no bearing on the conclusion. So,

$$S(k) \approx S^{(0)}(k) + S^{(1)}(k) + S^{(2)}(k) \quad (50)$$

$$S^{(0)}(k) = \frac{1}{\not{k}}, \quad S^{(1)}(k) = \frac{1}{\not{k}} (\not{b} \gamma^5) \frac{1}{\not{k}}, \quad S^{(2)}(k) = \frac{1}{\not{k}} (\not{b} \gamma^5) \frac{1}{\not{k}} (\not{b} \gamma^5) \frac{1}{\not{k}} \quad (51)$$

Thus

$$\Pi^{\mu\nu}(p; b) \approx \Pi_0^{\mu\nu} + \Pi_b^{\mu\nu} + \Pi_{bb}^{\mu\nu}$$

$\Pi_0^{\mu\nu}$ is standard GI ($\Pi_0^{\mu\nu} p_\mu = 0$) result. $\Pi_b^{\mu\nu}$ corresponds to a Chern–Simons-like term, which can appear GI in form ($\Pi_b^{\mu\nu} p_\mu = 0$). But $\Pi_{bb}^{\mu\nu}$ is not GI any more even in form. If we calculate

$$\begin{aligned} \Pi_{bb}^{\mu\nu} = & \int \frac{d^4 q}{(2\pi)^4} \text{Tr}[\gamma^\mu S^{(1)}(q) \gamma^\nu S^{(1)}(p-q) \\ & + \gamma^\mu S^{(2)}(q) \gamma^\nu S^{(0)}(p-q) + \gamma^\mu S^{(0)}(q) \gamma^\nu S^{(2)}(p-q)] \end{aligned} \quad (52)$$

we can check whether $p_\mu p_\nu \Pi_{bb}^{\mu\nu}$ is zero or not. If it is not a zero, then GI is broken. Only general form $\Pi_{bb}^{\mu\nu}$ can assume is the following

$$p_\mu p_\nu \Pi_{bb}^{\mu\nu} = A(p_\mu^2) p_\nu^2 b_\lambda^2 + B(p_\nu^2) (p^\mu b_\mu)^2 \quad (53)$$

while calculation of $A(p_\mu^2)$ and $B(p_\nu^2)$ is straightforward, it is rather lengthy. Therefore, we can simplify our task by putting p_ν on the mass shell ($p_\nu^2 = 0$). If GI is conserved, it should remain conserved on the mass shell as well. Applying the on-shell condition and symmetry properties of the integrals gives

$$p_\mu p_\nu \Pi_{bb}^{\mu\nu} = B(p_\nu^2) (p^\mu b_\mu)^2 = \frac{16}{3} (p^\mu b_\mu)^2 \int \frac{d^4 q}{(2\pi)^4} \frac{1}{(q_\mu^2)^2} \quad (54)$$

which shows explicitly that GI is broken.

References

- [1] AGASA Collab. (M. Takeda et al.). Extension of the Cosmic-Ray Energy Spectrum beyond the Predicted Greisen-Zatsepin-Kuz'min Cutoff. *Phys.Rev.Lett.* 81 (1998) 1163-1166. <https://doi.org/10.48550/arXiv.astro-ph/9807193>
- AGASA Collab. (M. Takeda et al.). Energy determination in the Akeno Giant Air Shower Array experiment. *Astropart.Phys.* 19 (2003) 447-462. <https://doi.org/10.48550/arXiv.astro-ph/0209422>
- [2] The Pierre Auger Collaboration. Features of the energy spectrum of cosmic rays above $2.5 * 10^{18}$ eV using the Pierre Auger Observatory. *Phys. Rev. Lett.* 125, 121106 (2020). <https://doi.org/10.48550/arXiv.2008.06488>
- The Pierre Auger Collaboration. Measurement of the cosmic-ray energy spectrum above $2.5 * 10^{18}$ eV using the Pierre Auger Observatory. *Phys. Rev. D* 102, 062005 (2020). <https://doi.org/10.48550/arXiv.2008.06486>

- The Pierre Auger Collaboration. The energy spectrum of cosmic rays beyond the turn-down around 10^{17} eV as measured with the surface detector of the Pierre Auger Observatory. *Eur. Phys. J. C* (2021) 81:966. <https://doi.org/10.48550/arXiv.2109.13400>
- [3] K.Greisen. End to the Cosmic-Ray Spectrum? *Phys. Rev. Lett.* 16, (1966) 748., <https://doi.org/10.1103/PhysRevLett.16.748> G.T. Zatsepin and V.A. Kuz'min. Upper limit of the spectrum of cosmic rays. *JETP Lett.* 41 (1966) 78
- [4] C. A. Moura, L. Quintino and F. Rossi-Torres. Analyzing the Time Spectrum of Supernova Neutrinos to Constrain Their Effective Mass or Lorentz Invariance Violation. *Universe* 9 (2023) no.6, 259. <https://doi.org/10.3390/universe9060259>
- [5] T. Jacobson, S. Liberati, D. Mattingly. Lorentz violation at high energy: concepts, phenomena and astrophysical constraints. *AnnalsPhys.*321:150-196,2006. <https://doi.org/10.48550/arXiv.astro-ph/0505267>
H. Martínez-Huerta, A. Pérez-Lorenzana. Effects of Lorentz invariance violation on cosmic ray photon emission and gamma ray decay processes. *PoS (ICRC2017)* 556. <https://doi.org/10.48550/arXiv.1709.08247>
P. Satunin. New constraints on Lorentz Invariance violation from Crab Nebula spectrum beyond 100 TeV. *Eur.Phys.J.C* 79 (2019) 12, 1011. <https://doi.org/10.48550/arXiv.1906.08221>
- [6] F. Duenkel, M. Niechciol, M. Risse. A new bound on Lorentz violation based on the absence of vacuum Cherenkov radiation in ultra-high energy air showers. *Phys. Rev. D* 107 (2023) 083004. <https://doi.org/10.48550/arXiv.2303.05849>
- [7] B. Altschul. Lorentz Violation and Synchrotron Radiation. *Phys.Rev. D*72 (2005) 085003. <https://doi.org/10.48550/arXiv.hep-th/0507258>
- [8] A. Kostelecky, N. Russell. Data Tables for Lorentz and CPT Violation. *Rev.Mod.Phys.* 83: 11 (2011). <https://doi.org/10.48550/arXiv.0801.0287>
- [9] S. Coleman, S. L. Glashow. High-Energy Tests of Lorentz Invariance. *Phys.Rev.D*59:116008,1999. <https://doi.org/10.48550/arXiv.hep-ph/9812418>
- [10] S. Chadha, H.B. Nielsen. Lorentz invariance as a low energy phenomenon. *Nuclear Phys. B* 217 (1983) 125. [https://doi.org/10.1016/0550-3213\(83\)90081-0](https://doi.org/10.1016/0550-3213(83)90081-0)
- [11] J.L. Chkareuli, C.D. Froggatt, H.B. Nielsen. Lorentz Invariance and Origin of Symmetries. *Phys. Rev. Lett.* 87 (2001) 091601. DOI: <https://doi.org/10.1103/PhysRevLett.87.091601>

- [12] J.L. Chkareuli, Z. Kepuladze, G. Tatishvili. Spontaneous Lorentz Violation via QED with Non-Exact Gauge Invariance. *Eur.Phys.J.C*55:309-316,2008. <https://doi.org/10.48550/arXiv.0802.1950>
 J.L. Chkareuli, J. Jejelava, Z. Kepuladze. Lorentzian Goldstone modes shared among photons and gravitons. *Eur.Phys.J.C* 78 (2018) 2, 156. <https://doi.org/10.48550/arXiv.1709.02736>
- [13] J.L. Chkareuli, Z. Kepuladze. Standard model with partial gauge invariance. *Eur. Phys. J. C* 72, 1954 (2012). <https://doi.org/10.1140/epjc/s10052-012-1954-9>
- [14] A. Kostelecky, C. Lane, A. Pickering. One-Loop Renormalization of Lorentz-Violating Electrodynamics. *Phys.Rev.D*65:056006,2002. <https://doi.org/10.48550/arXiv.hep-th/0111123>
 D. Anselmi, M. Halat. Renormalization of Lorentz violating theories. *Phys.Rev.D*76:125011,2007. <https://doi.org/10.48550/arXiv.0707.2480>
 J.R. Nascimento, A.Yu. Petrov, C.M. Reyes. Renormalization in a Lorentz-violating model and higher-order operators. *Eur. Phys. J. C* (2018) 78:541. <https://doi.org/10.48550/arXiv.1706.01466>
 S. Karki, B. Altschul. Renormalization Scheme Dependence of β -Functions In Lorentz-Violating Quantum Field Theory. *Eur. Phys. J. C* 82, 676 (2022). <https://doi.org/10.48550/arXiv.2110.08646>
- [15] J.L. Chkareuli, C.D. Froggatt, H.B. Nielsen. Deriving Gauge Symmetry and Spontaneous Lorentz Violation. *Nucl.Phys.B*821:65-73,2009. <https://doi.org/10.48550/arXiv.hep-th/0610186>
 J.L. Chkareuli, C.D. Froggatt, H.B. Nielsen. Spontaneously generated gauge invariance. *Nucl. Phys. B* 609 (2001) 46. [https://doi.org/10.1016/S0550-3213\(01\)00283-8](https://doi.org/10.1016/S0550-3213(01)00283-8)
- [16] R. Jackiw, A. Kostelecky. Radiatively Induced Lorentz and CPT Violation in Electrodynamics. *Phys.Rev.Lett.*82:3572-3575,1999. <https://doi.org/10.48550/arXiv.hep-ph/9901358>
- [17] B. Altschul. Failure of Gauge Invariance in the Nonperturbative Formulation of Massless Lorentz-Violating QED. *Phys.Rev. D*69 (2004) 125009. <https://doi.org/10.48550/arXiv.hep-th/0311200>
 B. Altschul. Gauge Invariance and the Pauli-Villars Regulator in Lorentz- and CPT-Violating Electrodynamics. *Phys.Rev. D*70 (2004) 101701. <https://doi.org/10.48550/arXiv.hep-th/0407172>
- [18] D.L. Anderson, M. Sher, I. Turan. Lorentz and CPT Violation in the Higgs Sector. *Phys.Rev. D*70 (2004) 016001. <https://doi.org/10.48550/arXiv.hep-ph/0403116>

- C.D. Carone, M. Sher, M. Vanderhaeghen. New Bounds on Isotropic Lorentz Violation. *Phys.Rev.D*74:077901,2006. <https://doi.org/10.48550/arXiv.hep-ph/0609150>
- B. Altschul. Bounds on Vacuum-Orthogonal Lorentz and CPT Violation from Radiative Corrections. *Phys. Rev. D* 99, 111701 (2019). <https://doi.org/10.48550/arXiv.1904.13042>
- [19] P. Satunin. One-loop correction to the photon velocity in Lorentz-violating QED. *Phys. Rev. D* 97, 125016 (2018). <https://doi.org/10.48550/arXiv.1705.07796>
- [20] A. Giarnetti, S. Marciano, D. Meloni. Exploring New Physics with Deep Underground Neutrino Experiment High-Energy Flux: The Case of Lorentz Invariance Violation, Large Extra Dimensions and Long-Range Forces. *Universe* 10 (2024) 9, 357. <https://doi.org/10.48550/arXiv.2407.17247>
- [21] Cheng-Gang Qin, Yu-Jie Tan, Xiao-Yu Lu, Tong Liu, Yan-Rui Yang, Qin Li, Cheng-Gang Shao. Constraints on violation of Lorentz symmetry with clock-comparison redshift experiments. *Physical Review D* 111 (2025) 055008 1-13. <https://doi.org/10.48550/arXiv.2503.13564>
- M.A. Hohensee, N. Leefer, D. Budker, C. Harabati, V.A. Dzuba, V.V. Flambaum. Limits on Violations of Lorentz Symmetry and the Einstein Equivalence Principle using Radio-Frequency Spectroscopy of Atomic Dysprosium. *Phys. Rev. Lett.* 111, 050401 (2013). <https://doi.org/10.48550/arXiv.1303.2747>
- [22] B. Altschul. Laboratory Bounds on Electron Lorentz Violation. *Phys. Rev. D* 82, 016002 (2010). <https://doi.org/10.48550/arXiv.1005.2994>
- [23] B. Altschul. Synchrotron and Inverse Compton Constraints on Lorentz Violations for Electrons. *Phys.Rev.D*74:083003,2006. <https://doi.org/10.48550/arXiv.hep-ph/0608332>
- [24] B. Altschul. Improved Bounds on Lorentz Symmetry Violation From High-Energy Astrophysical Sources. *Symmetry*13, 688 (2021). <https://doi.org/10.48550/arXiv.2104.04587>
- [25] H. Mueller, S. Herrmann, C. Braxmaier, S. Schiller, A. Peters. Modern Michelson-Morley experiment using cryogenic optical resonators. *Phys.Rev.Lett.*91:020401,2003. <https://doi.org/10.48550/arXiv.physics/0305117>
- [26] M. Kaku. Quantum field theory: A Modern introduction. Oxford university press. 1993.
- [27] O. Gagnon, G.D. Moore. Limits on Lorentz violation from the highest energy cosmic rays. *Phys.Rev. D*70 (2004) 065002. <https://doi.org/10.48550/arXiv.hep-ph/0404196>

- Floyd W. Stecker. Constraining Superluminal Electron and Neutrino Velocities using the 2010 Crab Nebula Flare and the Ice-Cube PeV Neutrino Events. *Astroparticle Physics* 56 (2014) 16. <https://doi.org/10.48550/arXiv.1306.6095>
- F. Duenkel, M. Niechciol, M. Risse. Photon decay in UHE air showers: stringent bound on Lorentz violation. *Phys. Rev. D* 104, 015010 (2021). <https://doi.org/10.48550/arXiv.2106.01012>
- [28] CMS Collaboration. Searches for violation of Lorentz invariance in top quark pair production using dilepton events in 13TeV proton-proton collisions. *Phys. Lett. B* 857 (2024) 138979. <https://doi.org/10.48550/arXiv.2405.14757>
- [29] E. Lunghi, N. Sherrill, A. Szczepaniak, A. Vieira. Quark-sector Lorentz violation in Z-boson production. *JHEP* 07 (2024) 167 (erratum). <https://doi.org/10.48550/arXiv.2011.02632>
- [30] ALEPH, DELPHI, L3, OPAL and SLD Collaborations, LEP EW Working Group and SLD EW and Heavy Flavour Groups: S. Schael et al. Precision Electroweak Measurements on the Z Resonance. *Phys.Rept.*427:257-454, 2006. <https://doi.org/10.48550/arXiv.hep-ex/0509008>
- [31] C. Hays [CDF]. High precision measurement of the W-boson mass with the CDF II detector. *PoS ICHEP2022*, 898 (2022). doi:10.22323/1.414.0898
- [32] [CMS]. Measurement of the W boson mass in proton-proton collisions at $\sqrt{s} = 13$ TeV, CMS-PAS-SMP-23-002.
ATLAS Collaboration, Improved W boson Mass Measurement using 7 TeV Proton-Proton Collisions with the ATLAS Detector, ATLAS-CONF-2023-004, CERN, Geneva, 2023.